AERODYNAMIC MECHANISM OF ACCORDION PITCH BENDING: SIMULATION AND THEORETICAL ANALYSIS

Seiji Adachi[1], Hyuga Okada[2], Toshiya Samejima[2], Masakazu Takeda[3], Kojiro Nishimiya[4]

[1] *School of Marine Science and Technology, Tianjin University, China*
[2] *Graduate School of Design, Kyushu University, Japan*
[3] *Department of Mechanical Engineering, Faculty of Science and Engineering, Otemon Gakuin University, Japan*
[4] *Faculty of Information Technology, Kanagawa Institute of Technology, Japan*

Abstract

The accordion is a free-reed instrument in which pitch bending can be achieved by forcefully operating the bellows while partially pressing a key. The pitch bending is primarily caused by the aerodynamic pressure loss at the vent hole of the reed chamber, which is partially opened by the pallet. The mechanism is fundamentally different from that of the harmonica, which relies on the player's vocal tract resonance. The flow constriction at the vent hole induces a significant pressure loss, causing the internal chamber pressure to fluctuate in synchronization with the reed vibration. This pressure fluctuation tends to close the reed strongly when it is near its closed position, but weakly when it is open, thereby partially offsetting the restoring force of the reed. This leads to a decrease in the effective spring constant and thus pitch bending. In this study, we first provide a qualitative explanation of this mechanism using an equivalent circuit and animation, and then present a physical model of accordion sound production. Through numerical simulations and theoretical nonlinear oscillation analysis, experimental results of pitch bending previously reported are reproduced.

Keywords: *free reed, equivalent circuit, pressure loss, physical modeling simulation, averaging method*

1. Introduction

To perform pitch bending on the accordion, the player forcefully operates the bellows while only partially pressing a key. This action lowers the pitch by up to approximately a semitone. Several experimental studies have reproduced this pitch bending [1], [2], [3]. These studies have observed changes in the bending depth, volume, and timbre, depending on factors such as the bellows direction (push or pull), the presence of a cassotto (a resonance box found in high-end accordions), and the size of the reed chamber. It has been revealed that pitch bending is accompanied by a decrease in volume, whereas the cassotto does not affect the pitch itself. However, no research has yet been published that elucidates the underlying generation mechanism of this pitch bending.

A pitch bending technique also exists for the harmonica. It has been demonstrated[4], [5] that the mechanism involves the player's vocal tract resonance. In this study, we report that the pitch bending mechanism of the accordion is fundamentally different from that of the harmonica.

2. Qualitative explanation

Figure 1 illustrates the internal structure of the accordion. On the side of the reed chamber, a pair of reeds tuned to the same pitch, corresponding to the push and pull of the bellows, is mounted via a reed plate. The reed chamber is normally closed by a pallet (valve); however, when a key is pressed, the pallet opens to create an airflow path. If the bellows are pulled while a key is pressed, the pressure inside the bellows decreases to $-p_0 < 0$. Air first flows into the reed chamber through the vent hole (pallet opening), which is open but somewhat constricted by the pallet, and then flows into the bellows through the gap between the pull reed and the reed plate (reed opening). In this manner, the airflow passes through two successive constrictions.

Constrictions introduce flow resistance, which causes the pressure within the reed chamber, $-p(t)$, to drop below the atmospheric pressure ($p = 0$). The reed vibrates while being sucked toward the bellows by the pressure difference between the upstream and downstream sides of the reed, $p_0 - p(t)$. Let R_p and

Corresponding author: *seiji_adachi@yahoo.co.jp.*

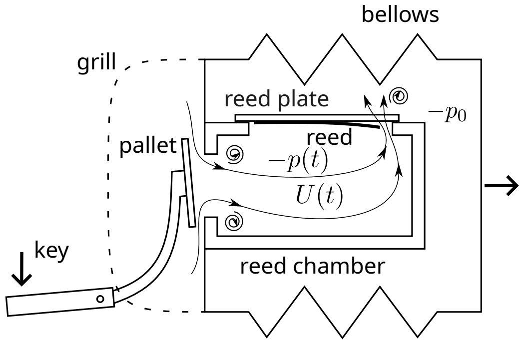

Figure 1: Internal structure of the accordion.

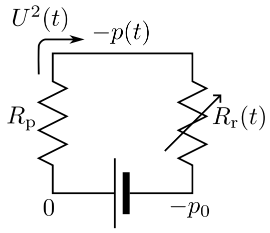

Figure 2: Equivalent circuit of the airflow in the accordion for the cases where the bellows are pulled.

$R_\mathrm{r}(t)$ be the flow resistances of the pallet and reed openings, respectively. Using the equivalent circuit in Fig. 2, we obtain

$$p_0 - p(t) = \frac{R_\mathrm{r}(t)}{R_\mathrm{p} + R_\mathrm{r}(t)} p_0. \tag{1}$$

By assuming a fixed pallet opening, R_p remains constant. On the other hand, $R_\mathrm{r}(t)$ is a resistance varying in time with the reed opening area during vibration. When the reed is pushed into the reed plate slot, $R_\mathrm{r}(t)$ becomes extremely large; hence, Eq. (1) indicates that $p_0 - p(t)$ is nearly equal to p_0. As the reed opens, $R_\mathrm{r}(t)$ decreases, which in turn lowers $p_0 - p(t)$. In other words, the sucking pressure $p_0 - p(t)$ tends to close the reed strongly when it is near the closed position and weakly when it is open. This force partially cancels the restoring force of the reed. Consequently, the effective spring constant of the reed decreases, thus resulting in pitch bending.

In the standard playing technique where a key is fully pressed, the pallet opening is large, making R_p small; in this case, $p_0 - p(t)$ remains relatively constant, resulting in negligible pitch bending. In the extreme case where $R_\mathrm{p} = 0$, the sucking pressure $p_0 - p(t) = p_0$ becomes constant, and no bending occurs. Conversely, when a key is only partially pressed, the pallet opening is small, which leads to a large R_p. Consequently, $p_0 - p(t)$ fluctuates significantly, making the pitch bending prominent. Figure 3(a) depicts the sucking pressure $p_0 - p(t)$ (blue arrow) and the restoring force (red arrow) for the case of $R_\mathrm{p} = 0$. In contrast, Fig. 3(b) illustrates these forces for a large R_p case. In the latter case, as the reed opens, the pressure in the reed chamber drops, thereby reducing the sucking pressure.

3. Review of the Reproduction Experiment

Okada et al. constructed an artificial blowing apparatus that simulates the internal structure of an accordion, and utilized it to experimentally reproduce pitch bending [6]. The key components of the apparatus are illustrated in Fig. 4. Upstream of the reed chamber, a front chamber is installed, into which air is supplied by a compressor. The pallet opening, defined by the distance L_p between the pallet and the vent hole, can be adjusted by a rod. Using this setup, a C4 reed was blown under two different pallet openings, $L_\mathrm{p} = \infty$ and 1 mm. The pitch of the generated sound was measured while systematically varying the blowing pressure p_0 inside the front chamber.

The experimental results are plotted in Fig. 5, where the fundamental frequency f is shown as a function of the blowing pressure p_0. The figure also displays the fitted lines obtained from the measured data. For both cases, $L_\mathrm{p} = \infty$ (blue) and 1 mm (orange), the pitch decreases almost linearly as the blowing pressure increases. The gradient for the former is $-2.5\,\mathrm{Hz/kPa}$, whereas that for the latter is $-5.1\,\mathrm{Hz/kPa}$. This indicates that the small opening yields the pitch-bending gradient roughly twice as steep as that of the large opening. The results reproduce the actual pitch bending which becomes more prominent when the player strongly manipulates the bellows while partially pressing a key.

4. Physical Model

The airflow entering through the pallet opening, passing through the reed chamber, and emerging out of the reed opening is assumed to be incompressible. Let $S(t)$ be the reed opening area, and $U(t)$ be the volume velocity of the airflow varying with $S(t)$. By considering the pressure drop due to flow velocity (Bernoulli effect), that caused by the flow separation at the constrictions, and the inertia of the lumped air passing through the reed opening, the extended Bernoulli equation becomes

$$\rho \frac{d}{S} \dot{U} = p_0 - K_\mathrm{p} \frac{\rho}{2} \left(\frac{U}{S_\mathrm{c}} \right)^2 - K_\mathrm{r} \frac{\rho}{2} \left(\frac{U}{S} \right)^2, \tag{2}$$

where ρ is the air density, S_c is the cross-sectional area of the reed chamber, and K_p and K_r represent the pressure loss coefficients at the pallet and reed openings, respectively. The lumped air is modeled as a "cylinder" with a cross-sectional area of $S(t)$ and a length along the flow direction of $d(t) = 0.5\sqrt{S(t)/\pi}$. The coefficient of 0.5 is determined to match with the experiment by Ricot et al. [7]

According to Idelchik [8], K_p increases as the pallet opening L_p decreases, and is expected to vary significantly from approximately unity to several hundreds. While K_r is typically around 2.7 for a circular orifice,

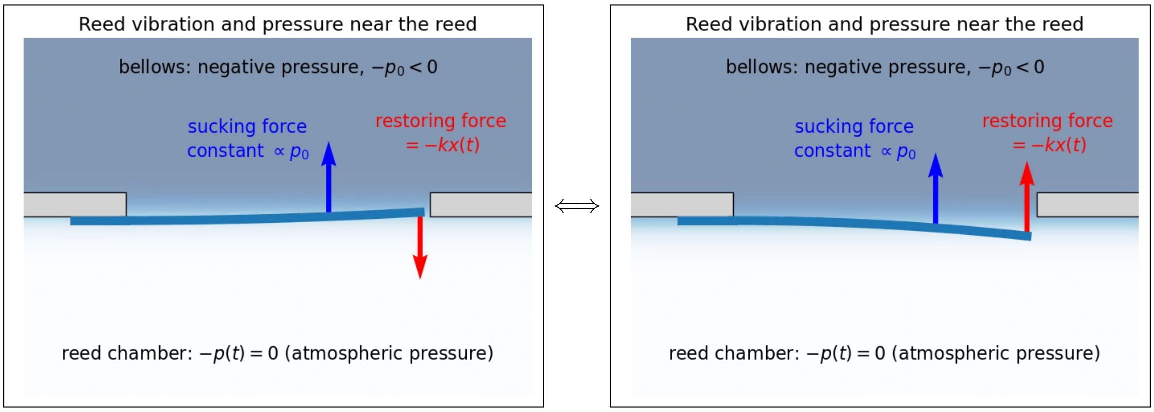

(a) $R_\mathrm{p} = 0$ case

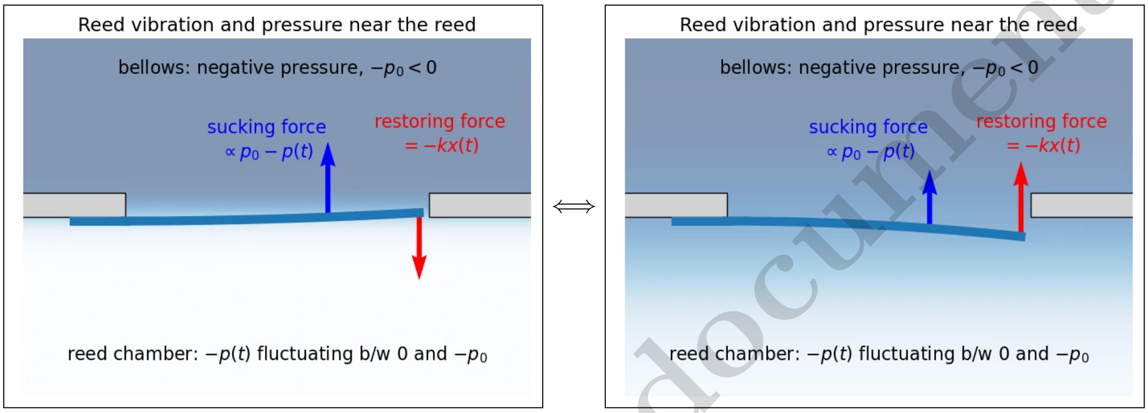

(b) Large R_p case

Figure 3: Comparison of the variations in the sucking force (blue arrow) and the reed restoring force (red arrow) for (a) the $R_\mathrm{p} = 0$ case and (b) the large R_p*case*. In the latter case, the resultant force of the sucking force and the inherent restoring force weakens, which reduces the effective spring constant and thus causes pitch bending.

it becomes much larger for highly flat geometries such as a reed opening. The first two terms on the right-hand side of Eq. (2) correspond to the pressure within the reed chamber,

$$p(t) = p_0 - K_\mathrm{p}\frac{\rho}{2}\left(\frac{U}{S_\mathrm{c}}\right)^2. \tag{3}$$

Note that the flow resistances used in Sec. 2 are $R_\mathrm{p} = K_\mathrm{p}\rho/(2S_\mathrm{c}^2)$ and $R_\mathrm{r} = K_\mathrm{r}\rho/(2S^2)$.

The reed tip displacement, $x(t)$, is assumed to follow the equation of motion of a simple one-degree-of-freedom spring-mass-damper system. The direction of the displacement is defined as positive toward the reed chamber, and $x = 0$ corresponds to the position where the reed is perfectly flush with the reed plate. The reed opening area $S(t)$ can then be

$$S(x) = (L + W)\sqrt{\max(x, 0)^2 + a^2}, \tag{4}$$

where L and W denote the length and width of the reed, respectively, and a represents the gap between the reed and the reed plate.

The reed is driven by aerodynamic forces, leading to self-sustained oscillations [7]. The pressure

$$p_\mathrm{r} = p(t) - \rho\frac{d(x)}{S(x)}\dot{U} = K_\mathrm{r}\frac{\rho}{2}\left(\frac{U}{S(x)}\right)^2 \tag{5}$$

is exerted on the upstream side of the reed. The inertial term in Eq. (5) represents a reaction force caused by the lumped air.

The downstream side of the reed is exposed to the open air, where the sound pressure $p_\mathrm{out}(t)$ radiates. Since $p_\mathrm{out}(t)$ is small compared to the pressure fluctuation of $p_\mathrm{r}(t)$, it can be omitted when analyzing the reed dynamics. Let M be the effective mass of the reed, ω_0 be its angular eigenfrequency, and ζ be the damping ratio. The equation of motion for the reed is

$$\ddot{x} = -\omega_0^2(x - x_\mathrm{rest}) - 2\zeta\omega_0\dot{x} - \frac{S_\mathrm{r}}{M}p_\mathrm{r}(t), \tag{6}$$

where $S_\mathrm{r} = LW$ represents the surface area of the reed, and x_rest denotes the equilibrium (rest) position.

The acoustic radiation impedance is inertive in the low-frequency range. The output sound pressure $p_\mathrm{out}(t)$

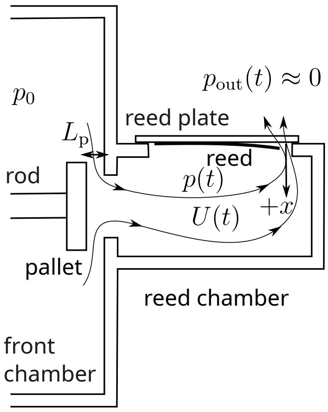

Figure 4: Experimental setup used for reproducing accordion pitch bending by Okada et al. [6] Only the main components are shown.

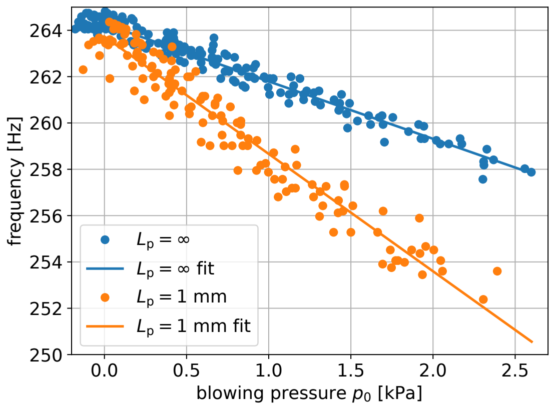

Figure 5: Accordion sound frequency as a function of the blowing pressure p_0. The blue dots and line show the results for the large pallet opening $L_\mathrm{p} = \infty$, while the orange ones show those for the small $L_\mathrm{p} = 1\,\mathrm{mm}$.

can then be evaluated from $U(t)$ with

$$p_\mathrm{out}(t) = \frac{\rho \Delta L}{S_\mathrm{r}} \dot{U}, \tag{7}$$

where $\Delta L = \sqrt{S_\mathrm{r}/\pi}$ represents the end correction for the radiation.

5. Numerical Simulation

The sound production of the accordion can be simulated by numerically solving Eqs. (2) and (6), which govern the volume velocity $U(t)$ of the airflow and the reed displacement $x(t)$. The parameters required for the simulation were determined based on the actual dimensions of the reed chamber and the measurement data of the reed. These are summarized in Table 1.

Figure 6 shows the steady-state waveforms simulated with a blowing pressure of $p_0 = 1\,\mathrm{kPa}$ and pressure loss coefficients of $K_\mathrm{p} = 35.0$ and $K_\mathrm{r} = 8.0$. When the reed is about to close, a sharp peak occurs in

Table 1: Simulation parameters

Name	Value
Air density ρ	$1.17\ \mathrm{kg/m^3}$
Reed eigenfreq. $\omega_0/(2\pi)$	267.6 Hz
Reed mass M	$(2/3) \times 0.248$ g
Reed damp. ratio ζ	0.003
Reed length L	32.8 mm
Reed width W	3.45 mm
Reed-plate gap a	0.14 mm
Reed disp. at rest x_rest	0.3 mm
Reed ch. x-sect. S_c	$14.8 \times 14.6\ \mathrm{mm}^2$

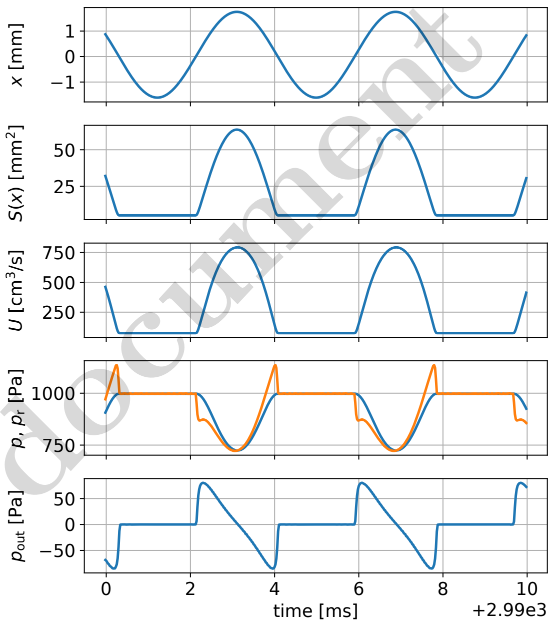

Figure 6: Simulated steady-state waveforms with the blowing pressure $p_0 = 1\,\mathrm{kPa}$ and the pressure loss coefficients $K_\mathrm{p} = 35.0$ and $K_\mathrm{r} = 8.0$. The sounding frequency is 265.1 Hz, showing a pitch drop of 2.5 Hz or 0.9 %.

the upstream pressure p_r, pushing the reed outward. Immediately after the reed opens, a dip appears in p_r, pulling the reed toward the reed chamber side. The resulting sounding frequency is 265.1 Hz, which exhibits a pitch drop of 2.5 Hz (or 0.9 %) from the eigenfrequency of the reed.

When the pressure loss coefficient at the pallet opening is increased to $K_\mathrm{p} = 150.0$, while the blowing pressure p_0 and the pressure loss coefficient at the reed opening K_r remain the same, the reed vibration amplitude decreases. The sounding frequency also decreases to 261.7 Hz, which results in a pitch drop of 5.9 Hz (or 2.2 %).

The simulated reed amplitudes and sounding frequencies during steady-state oscillation are plotted in Fig. 7 as functions of the blowing pressure p_0. As p_0 increases, the amplitude monotonically increases, whereas the frequency monotonically decreases. The

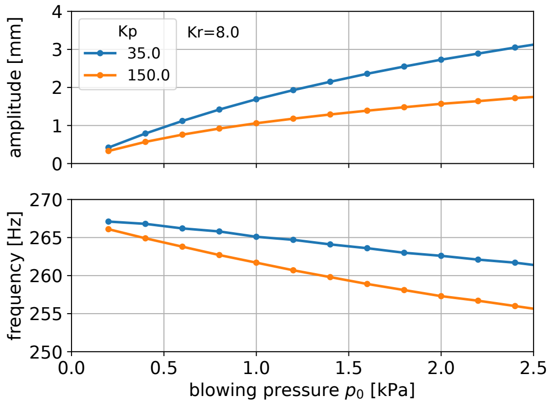

Figure 7: Amplitudes (upper) and frequencies (lower) simulated for the small $K_\mathrm{p} = 35.0$ and the large $K_\mathrm{p} = 150.0$ as functions of the blowing pressure p_0. K_r is fixed to 8.0.

pitch-bending gradient between 0 and 1 kPa are −2.5 Hz/kPa for $K_\mathrm{p} = 35.0$ and −5.9 Hz/kPa for $K_\mathrm{p} = 150.0$. Although the simulated frequencies are overall 2 to 3 Hz higher than those measured experimentally, the results are in good agreement with the characteristic pitch-bending behavior observed in Fig. 5.

6. Theoretical Analysis

The pitch-bending behavior can be analytically derived using the Krylov-Bogoliubov averaging method [9] with a few simplifications. The inertia of the lumped air is assumed to be constant and independent of the instantaneous reed displacement. The equilibrium position x_rest is assumed to be sufficiently small compared to the dynamic reed displacement $x(t)$ and is thus neglected. The gap a between the reed and the reed plate is also assumed to be negligibly small, yielding the simplified opening area relation $S(x) = (L + W)\max(0, x)$.

By taking the blowing pressure p_0 as a reference, the characteristic length of the system is defined as $x_0 = S_\mathrm{r} p_0/(M\omega_0^2)$, which represents the static displacement of the reed under a uniform pressure p_0. Similarly, the characteristic velocity, area, volume velocity, and time scale are defined as $v_0 = \sqrt{2p_0/\rho}$, $S_0 = S(x_0)$, $U_0 = S_0 v_0$, and $T = 1/\omega_0$, respectively. We then introduce the following dimensionless variables: time $\tilde{t} = t/T$, reed displacement $X(\tilde{t}) = x(t)/x_0$, volume velocity $Y(\tilde{t}) = \sqrt{K_\mathrm{r}}U(t)/U_0$, and reed opening area $S(X) = S(x)/S_0 = \max(0, X)$. Under these definitions, $X(\tilde{t})$ and $Y(\tilde{t})$ satisfy the coupled dimensionless equations,

$$\ddot{X} + X = -2\zeta\dot{X} - \frac{Y^2}{S^2(X)}, \tag{8}$$

$$\alpha\dot{Y} = 1 - \beta Y^2 - \frac{Y^2}{S^2(X)}, \tag{9}$$

where the right-hand side of Eq. (8) is abbreviated as $G(X, Y)$. Here, α and β are dimensionless parameters associated with the inertia of the lumped air at the reed opening and the ratio of pressure loss coefficients, respectively. These are

$$\alpha = \frac{2\bar{d}\omega_0 S_0}{\sqrt{K_\mathrm{r}}v_0\bar{S}}, \quad \beta = \frac{K_\mathrm{p}}{K_\mathrm{r}}\frac{S_0^2}{S_\mathrm{c}^2}. \tag{10}$$

Note here that $\alpha \ll 1$ and $\beta \lesssim 1$.

To obtain the approximate solutions of Eqs. (8) and (9), we assume that the dimensionless displacement $X(\tilde{t})$ takes the following form (ansatz):

$$X(\tilde{t}) = A\sin(\tilde{t} + \phi), \quad \dot{X}(\tilde{t}) = A\cos(\tilde{t} + \phi), \tag{11}$$

where the amplitude A and the phase ϕ are also functions of the dimensionless time $\tilde{t}$. They are assumed to vary sufficiently slowly compared to the dimensionless eigenfrequency of the reed, which is equal to unity. The total phase is abbreviated as $\theta = \tilde{t} + \phi$. Substituting Eq. (11) into Eq. (8) yields the amplitude and phase equations,

$$\dot{A} = \langle G(X, Y)\cos\theta\rangle, \quad \dot{\phi} = -\frac{1}{A}\langle G(X, Y)\sin\theta\rangle. \tag{12}$$

Since A and ϕ remain practically constant over a single oscillation cycle, the right-hand sides of these equations have been averaged over one period.

To solve Eq. (12), it is first necessary to express Y as a function of X. By solving Eq. (9) perturbatively in powers of α, we obtain

$$Y = \frac{S(X)}{\sqrt{1 + \beta S^2(X)}} - \frac{\alpha}{2}\frac{S(X)\dot{S}(X)}{\left[1 + \beta S^2(X)\right]^2} + \cdots, \tag{13}$$

where the first term on the right-hand side represents an effect of squaring the volume velocity waveform $U(t)$, and the second term accounts for a slight phase delay in the oscillation. Substituting this expression into $G(X, Y)$ yields

$$G(X) \equiv G(X, Y) = -2\zeta\dot{X} - \frac{1}{1 + \beta S^2(X)} + \alpha\frac{\dot{S}(X)}{\left[1 + \beta S^2(X)\right]^{5/2}} + \cdots. \tag{14}$$

The second term on the right-hand side of Eq. (14) corresponds to the dimensionless pressure waveform inside the reed chamber. The third term represents the sharp pressure peak immediately before the reed closes and the dip right after it opens.

Evaluating Eq. (12) using the expanded expression for $G(X)$ in Eq. (14) yields

$$\dot{A} = -\zeta A + \frac{\alpha A}{4}\,{}_2F_1\!\left(\frac{5}{2}, \frac{1}{2}, 2; -\beta A^2\right), \tag{15}$$

$$\dot{\phi} = \frac{1}{\pi A}\left[\frac{\operatorname{atanh}\sqrt{\beta A^2/(1 + \beta A^2)}}{\sqrt{\beta A^2(1 + \beta A^2)}} - 1\right], \tag{16}$$

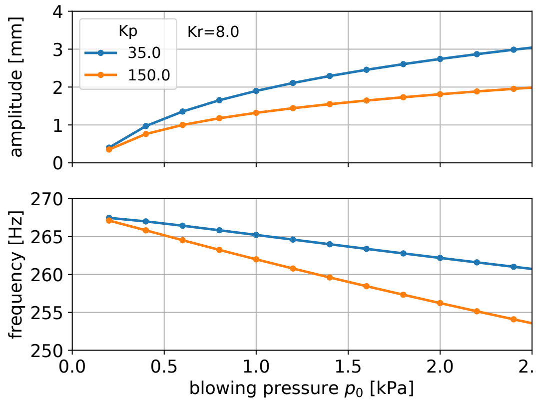

Figure 8: Amplitudes (upper) and frequencies (lower) estimated for the small $K_\mathrm{p} = 35.0$ and the large $K_\mathrm{p} = 150.0$ as functions of the blowing pressure p_0. K_r is fixed to 8.0.

where ${}_2F_1(a, b, c; z)$ denotes Gauss's hypergeometric function [10].
When $A \ll 1$, Eq. (15) simplifies to $\dot{A} = (-\zeta + \alpha/4)A$. Consequently, the threshold condition for the reed to initiate oscillation is given by $\alpha > 4\zeta$. This is satisfied when the blowing pressure p_0 is approximately 200 Pa or higher.
In the steady state after the oscillation has fully developed, the amplitude growth ceases ($\dot{A} = 0$). Thus, Eq. (15) immediately yields the steady-state relation,

$$ {}_2F_1\left(\frac{5}{2}, \frac{1}{2}, 2; -\beta A^2\right) = 4\frac{\zeta}{\alpha}. \tag{17}$$

By numerically solving Eq. (17) for a given set of parameters, the steady-state vibration amplitude A^* can be uniquely determined. Meanwhile, the dimensionless sounding frequency is defined by the total phase velocity as

$$\frac{d\theta}{d\tilde{t}} = 1 + \dot{\phi} = \frac{\omega}{\omega_0}. \tag{18}$$

By substituting the determined steady-state amplitude A^* into $\dot{\phi}$ in Eq. (16), the rate of the pitch drop can be explicitly evaluated.
Figure 8 shows the steady-state vibration amplitudes and sounding frequencies predicted by the theoretical analysis. The estimated pitch-bending gradient between 0 and 1 kPa are -2.4 Hz/kPa for $K_\mathrm{p} = 35.0$ and -5.6 Hz/kPa for $K_\mathrm{p} = 150.0$. Consistent with the numerical simulation results, the theoretical analysis based on the averaging method also well explains the experimental trends of the pitch-bending behavior.

7. Conclusion

The pitch-bending behavior in the accordion is primarily caused by the pressure loss of the airflow passing through the pallet opening. To best reproduce the experimental results, it was found that the pallet pressure loss coefficient was set to $K_\mathrm{p} = 35.0$ for a large pallet opening, and increased to $K_\mathrm{p} = 150.0$ for a small pallet opening. The reed opening pressure loss coefficient was set to $K_\mathrm{r} = 8.0$ in both cases.
In future work, we plan to conduct detailed experiments to measure the actual pressure loss coefficients. By comparing the experimentally measured values with the calibrated parameters used in this study, we aim to further validate the accuracy and robustness of the proposed physical model.

References

[1] R. Llanos-Vazquez, M. J. Elejalde-García, and E. Macho-Stadler, "Controllable pitch-bending effects in the accordion playing," in *Proc. of the Acoustics '08 Paris (Joint meeting of the 155th ASA Meeting, 5th Forum Acusticum, and 9th SFA Convention)*, Paris, France, 2000, pp. 4437–4442.

[2] W. L. Coyle, S. L. Behrens, and J. P. Cottingham, "Influence of accordion reed chamber geometry on reed vibration and airflow," *J. Acoust. Soc. Am.*, vol. 126, 2216(A), 2009.

[3] J. P. Cottingham, "Pitch bending and multiple-mode reed vibration in mechanically-blown free reed instruments," in *Proc. of the International Symposium on Music Acoustics (ISMA 2010)*, Sydney and Katoomba, Australia, 2010, paper No. 28.

[4] R. B. Johnston, "Pitch control in harmonica playing," *Acoustics Australia*, vol. 15, no. 3, pp. 69–75, 1987.

[5] S. Adachi, H. Okada, T. Samejima, and K. Nishimiya, "Time-domain simulation of harmonica pitch bending and overblowing," *J. Acoust. Soc. Am.*, vol. 159, no. 1, pp. 4191–4203, 2026.

[6] H. Okada, K. Nishimiya, and H. Cho, "Pitch bending in accordions: Observation and considerations," *J. Acoust. Soc. Jpn.*, vol. 81, no. 11, pp. 739–742, 2025, (in Japanese).

[7] D. Ricot, R. Caussé, and N. Misdariis, "Aerodynamic excitation and sound production of blown-closed free reeds witout acoustic coupling: The example of the accordion reed," *Journal of the Acoustical Society of America*, vol. 117, no. 4, pp. 2279–2290, 2005.

[8] I. E. Idelchik, *Handbook of Hydraulic Resistance*, 4th ed. rev. and augmented, A. S. Ginevskiy and A. V. Kolesnikov, Eds. New York: Begell House, 2007, Translated by G. R. Malyavskaya and N. K. Shveyeva.

[9] N. H. Fletcher and T. D. Rossing, *The Physics of Musical Instruments*, 2nd. New York: Springer, 1998, ch. 5, pp. 134–136, Sec. 15.1.

[10] NIST Digital Library of Mathematical Functions, *Release 1.2.6*, Chap. 15, `https://dlmf.nist.gov/15`, 2026.